Desalination and Water Treatment
www.deswater.com

doi:10.5004/dwt.2019.23877

148 (2019) 374–379
April

Synthesis and adsorption studies of alumina-silicate hybrid for remediation of mercury and lead

Fatima Tariq*, Uzaira Rafique

Department of Environmental Sciences, Fatima Jinnah Women University, The mall, Rawalpindi, Pakistan, Tel. +923215525563, email: Fatimatariq86@gmail.com (F. Tariq), uzairaiqbal@yahoo.com (U. Rafique)

Received 11 October 2018; Accepted 27 January 2019

ABSTRACT

Alumina-silicate based hybrid has significant physicochemical properties with a great potential application to remove toxic pollutants from different compartment i.e., air, water and soil of the environment. Mercury and lead stated as recalcitrant pollutants and need special treatment for removal from environmental media. Inspite of peculiar features of alumina-silicate, it offers certain limitations regarding synthetic cost using expensive precursor and solvents. The present research is an attempt to synthesize the cost-effective alumina-silicate hybrid using aluminum nitrate and sodium silicate for the removal of mercury and lead. IR confirmed the formation of a hybrid through shifting of absorption peaks at a higher intensity. SEM showed hexagonal shaped particles while XRD pattern showed semi-crystalline phase with FWHM = 0.29, 2θ = 18.11, d spacing = 4.9 and 50 nm particle size calculated through well-known Scherrer equation. XPS survey scan showed all respective elements i.e., silicon (109.9 eV), aluminum (78.6 eV), and oxygen (530 eV). Nitrogen adsorption-desorption isotherm reveals reduced surface area and porosity thus, enhanced ion exchangeable capacity. Adsorption experiment showed 69% of Lead removal and 66% of Mercury removal within 120 min. Hence, it provides an alternate option for the cost-effective synthesis of alumina-silicate.

Keywords: Alumina-silicate; Hybrid; Lead; Mercury; Adsorption

1. Introduction

Alumina-silicate considered as remarkable material due to its physiochemical properties such as the high surface area to volume ratio, high mechanical and chemical stability, good catalytic and ion exchange ability. In past, alumina-silicate was synthetically designed on the basis of source, method and physiochemical property. Electrochemical anodization [1] is widely used method for synthesizing free-standing silica and alumina-silicate nano-bottles [2], graphene and alumina hybrid [3] and even alumina membrane, by varying the electrolytes (e.g. sulphuric acid, phosphoric acid and oxalic acid) and anodizing potential. Addition of sulphuric acid offered much smaller pore volume in comparison to oxalic acid and phosphoric acid. The resulted small pore volume is efficiently applied for filtration and catalysis application [4]. The growth behavior of anodic oxide films by acid dissociation of anodizing alumina under various electrochemical condition affected by varying glutaric acid concentration [5]. The effect of altering anodizing condition in the fabrication of ordered porous anodic alumina at ultrahigh voltages (600–800 V) and a series of mixed electrolytes i.e., citric acid, ethylene glycol and phosphoric acid solutions are also reported by Chen et al. [6]. Bismuth and zinc oxide hybrid [7] synthesized by anodization affected the surface and pore structure of the material. Similarly, titanium oxide coated with zinc by applying thermal evaporation technique coupled with hydrothermal to decorate the nano-bottles with zinc oxide nano-tip [8]. In an addition to that, Wang et al. [9] reported the synthesis of alumina and alumina-silicate for effective removal of congo red from textile wastewater. Cai et al. [10] reported the synthesis of alumina nano-flakes using thiourea as a precipitating agent for efficient adsorption of phenol as well as for capturing carbon dioxide. However,

*Corresponding author.

these conventional techniques haven't gained wide acceptance due to high cost, sophisticated setup considered as a non-economical route of synthesis. The limitation associated with synthesis technique led to the continuous development of new method and advancement in techniques ranging from complex to simple. The present study is an endeavor toward the synthesis of alumina-silicate using simple, economical and an environmentally viable mean i.e., sol-gel. The material will serve as an efficient adsorbent for remediation of noxious Lead and Mercury [11,12].

2. Experimental details

2.1. Reagents

Aluminium nitrate nonahydrate (>99.99%) and Sodium silicate (>99.99%) were purchased from Riedel-de-Haen. Cetyl tri-methyl-ammonium chloride (CTAC) was acquired from BDH, while Sigma Aldrich provided Lead (>99.99%), and Mercury (>99.99%). All chemicals used were of the analytical reagent grade.

2.2. Synthesis of Alumina-silicate

The present research work provided a cost-effective and successful synthesis method for alumina-silicate hybrid [13]. The adapted sol-gel proven to be an economical alternate approach for electrochemical anodization. Furthermore, use of sodium silicate and aluminum nitrate nonahydrate in place of expensive chemicals such as TEOS and impure boehmite (aluminum oxide hydroxide) [14] are also added advantages.

For synthesis, an equivalent (1:1) ratio of aluminium nitrate and sodium silicate were liquefied in 96 mL of deionized water and 0.9 mL of 2 M NaOH. The mixture was stirred and heated at 90°C for 2 h with the addition of 5 ml of cetyltrimethyl ammonium chloride (CTAC). The crude product was, washed, filtered and calcined at 700°C for 4 h [15]. The scheme of synthesis is presented in Fig. 1.

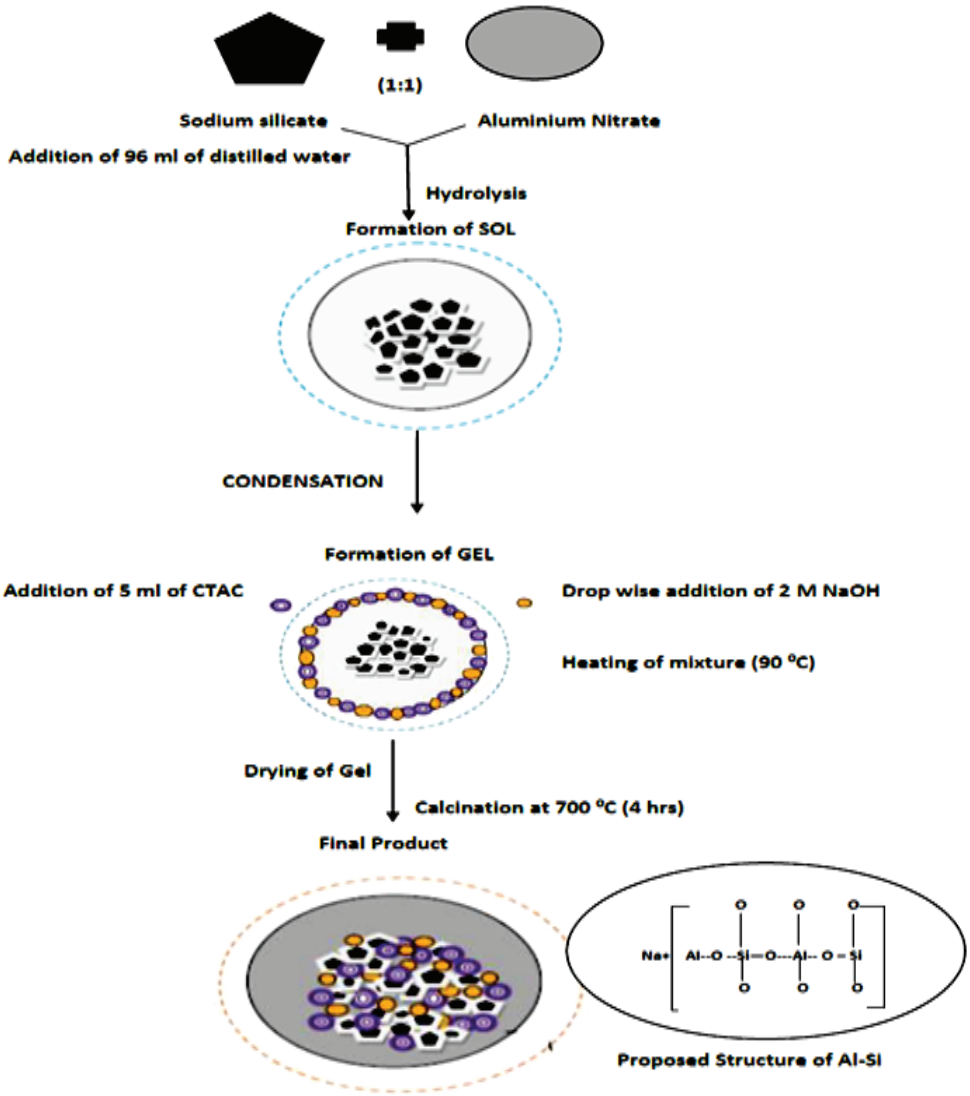

Fig. 1. Scheme for synthesis of alumina-silicate hybrid.

It is proposed that synthesis followed suspension and gel formation resulting in development of symmetric structure having interactions between strong acidic (OH) and weak acidobasic sites (O^-Na^+). The Na^+ ions act as anion exchanger and therefore, bind proficiently with metal ions in solution [16].

2.3. Batch adsorption

The efficacy of as-synthesized hybrid material was evaluated using batch adsorption experiment for removal of mercury and lead by keeping the dose constant (10 mg/kg). For this purpose, 1000 mg/L stock solutions of each metal were subjected to prepare different induced concentrations (30, 50 and 70 mg/L). The contact of alumina-silicate (adsorbent) and metal (adsorbate) was made for time period of 120 min by placing on the shaker (Lab-companion SK-300). An aliquot was drawn after regular time intervals, filtered and analyzed on standardized Atomic Absorption Spectrophotometer (AA 220, Varian). The adsorbed metal concentration on synthesized hybrid was calculated by Eq. (1):

$$q_e = \left(\frac{C_i - C_t}{W}\right)V \quad (1)$$

where C_i and C_t (mg/L) are the liquid- phase concentrations of adsorbate initially and at interval time t, respectively. V is the volume (mL) of the solution and W is the weight (mg/L) of adsorbent. Removal of metals (%R) by the synthesized alumina-silicate was calculated from the relation given in Eq. (2):

$$\%R = \left(\frac{C_i - C_t}{C_i}\right)100 \quad (2)$$

3. Results and discussion

3.1. Characterization

The as-synthesized alumina-silicate material was characterized using standard analytical techniques such as Fourier transform infrared spectroscopy (FTIR-8400 Schimadzu, Japan), X-ray diffraction (STOE), scanning electron microscopy (JEOL tsm-6490, Japan), X-ray photoelectron spectroscopy (Thermo K-alpha spectrometer) and Brunauer, Emmitt and Teller (BET-Quadra Sorb-QS oncom1). The working condition of each respective techniques is given as.

Standard KBr pellet method was used to record the spectrum of alumina-silicate from 4000–400 cm^{-1}. Gold sputtering was performed on alumina-silicate take SEM images and analyzed on 5 kV at 6.5 mm. Monochromatic AlKa X-ray as excitation source at an energy range of 50–20 eV with a step size of 0.1 eV and dwell time of 1000 ms. The pressure inside the chamber was kept between 1.23×10^{-6}–1.31×10^{-7} Pa during XPS analysis. Cu K α radiation (λ = 1.5405) was used for XRD analysis from 10–71° by a step size of 0.01.BET (Quadra sorb-QS $oncom^{-1}$) by taking 0.2 g of a sample for single measurement under nitrogen environment.

3.2. FTIR analysis

IR spectrum (Fig. 2) indicated characteristic peaks of silica, alumina and alumina-silicate hybrid. The broad peak at 3405 cm^{-1} assigned to OH represented the physisorbed water from the atmosphere [17]. The peak at 465 cm^{-1} assigned to Si-O-Si of silica [18] while 786 cm^{-1} assigned to tetra coordinated binding (Al-O-Al) of alumina [19]. The emergence of a new peak at 1102 cm^{-1} suggested successful synthesis of hybrid resulted from bridging of Si-O-Al via replacement of Si with Al atoms [20].

3.3. SEM analysis

Fig.3 shows hexagonal shaped structure stacked onto one another and created large void spaces [21] resulting in the formation of alumina-silicate matrix. It is also speculated that these void spaces provided the surface platform for adsorption of lead (Pb) and mercury (Hg).

3.4. XPS analysis

XPS survey scan (Fig. 4) of alumina-silicate confirmed the presence of oxygen, aluminium, and silicon in as-synthe-

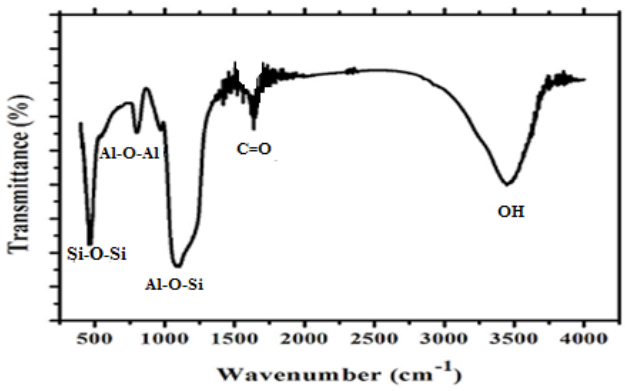

Fig. 2. IR spectrum of alumina-silicate hybrid.

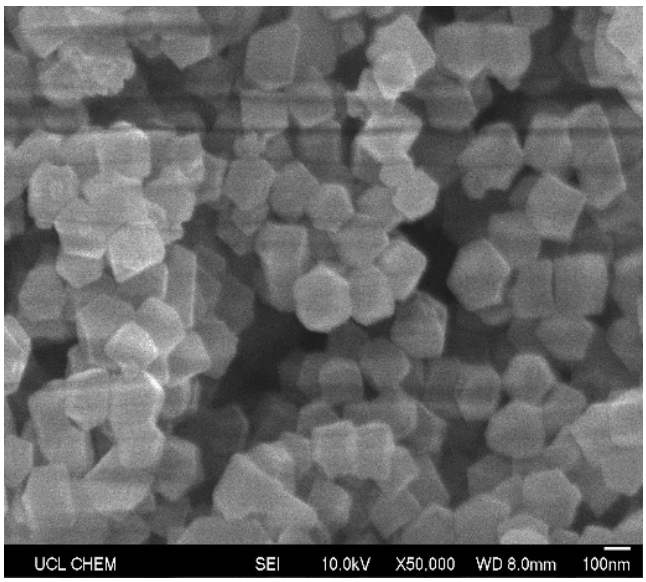

Fig.3. SEM image of alumina-silicate hybrid.

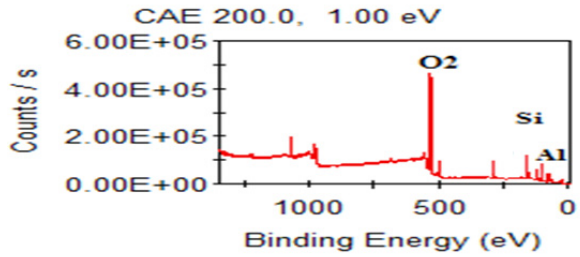

Fig. 4. XPS survey scan of alumina-silicate hybrid.

Table 1
XPS data of alumina-silicate

Name	Start BE	Peak BE	End BE	Height CPS	Atomic %
Si2p	109.9	102.9	95.10	524.5	34.2
Al2p	78.70	74.90	71.90	629.3	20.07
O1s	511.6	530.1	93.6	2.07	45.73

sized hybrid at 530 eV, 78.7 eV, and 109.9 eV, respectively. The appearance of aluminium and oxygen peak is attributed to unreacted aluminium salt precursor [22]. The core level scan of Si and Al, shown in Table 1 suggested 2p hybridization closely spaced spin-orbit based on its symmetric (low pass energy) and asymmetric components (higher pass energy).

3.5. XRD analysis

XRD pattern revealed the semi-crystalline nature of alumina-silicate hybrid as shown in Fig. 5. A distinct new peak at 2θ = 18.11 with d-spacing = 4.9 suggested interconnectivity of silica and alumina with four oxygen atoms [23]. The XRD data speculated a=b=c=23.72 Å, α=β=γ=90°, with the space group of Fn3c (237). The average particle size of 50 nm was calculated using Debye Scherer's equation ($D = 0.94\lambda / \beta\cos\theta$).

3.6. Nitrogen adsorption-desorption isotherm

The N_2 adsorption-desorption isotherm of alumina-silicate hybrid (Fig. 6) depicted adsorption as type III, based on International Union of Pure and Applied Chemistry (IUPAC) classification system in 1985 [24]. This peculiar adsorption is characterized by stronger interaction of adsorbate with an adsorbed layer rather than adsorbent surface. The formation of alumina-silicate hybrid was further confirmed by significant reduction in surface area (11.786 m^2/g) and pore volume (4.7 cm^3/g) in comparison to individual silica (573 m^2/g) and alumina (631 m^2/g) supported by literature [25]. Furthermore, the particular calcination temperature also affected the pore structure and surface area of alumina-silicate [26].

3.7. Adsorption of Mercury and Lead

The adsorption trend of two toxic metals (Pb and Hg) as a function of time and concentration are presented in Figs. 7a and b. The increase in adsorption of metals with an

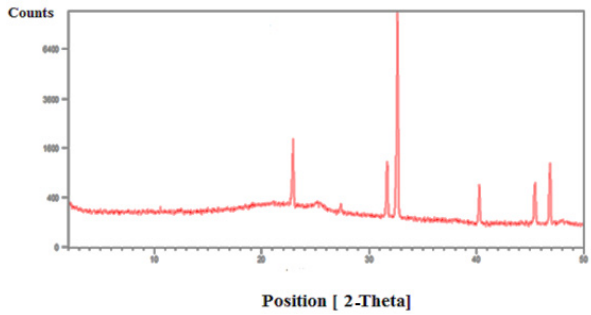

Fig. 5. XRD pattern of alumina-silicate hybrid.

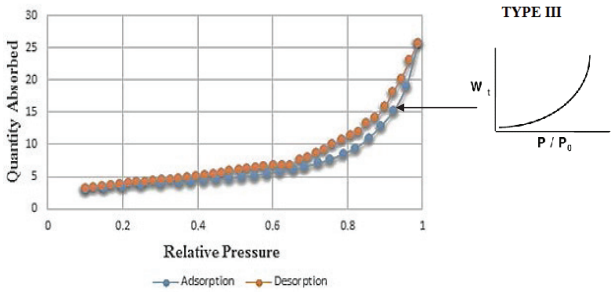

Fig. 6. Nitrogen isotherm of alumina-silicate hybrid.

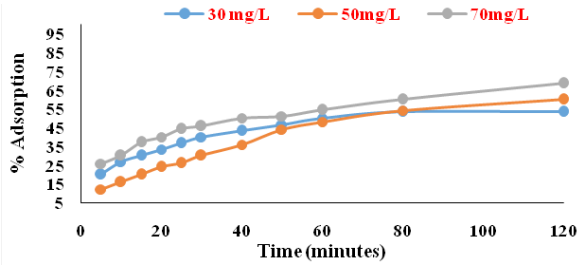

(a)

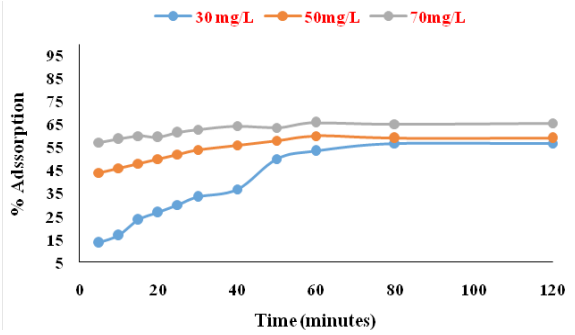

(b)

Fig. 7. Adsorption of (a) Lead and (b) Mercury as a function of time and concentration.

increase in time was due to available active sites on the surface of hybrid and incorporation of incoming ions between void spaces. The attainment of equilibrium after 60 min indicated filling up of spaces leading to saturation and ces-

sation of the adsorption process. The optimum adsorption of Pb (69%) and Hg (66%) was achieved at 70 mg/L [27] with appreciable adsorption capacity at lower concentrations (i.e., 30 mg/L and 50 mg/L). The trend followed as:

Pb: 70 mg/L (69%) > 50 mg/L (60%) > 30 mg/L (53%)

Hg: 70 µg/L (66%) > 50 µg/L (59%) > 30 µg/L (57%)

3.8. Adsorption kinetics

Adsorption kinetics and isotherm models give insight information about adsorption rate and mechanism. Adsorption kinetics (pseudo-first, second, and intra-particle diffusion), and adsorption isotherms (Langmuir and Freundlich isotherm) were applied on experimental data. The regression coefficients (R^2) value (shown in Figs. 8 and 9) and (summarized in Table 2) indicated good fitness of pseudo-second order (0.98) and Freundlich isotherm (0.97) suggesting heterogeneous multi-layered adsorption. Closeness between experimental and calculated adsorption capacity (q_e) also confirmed fitness of pseudo-second order kinetics.

4. Conclusions

The physicochemical properties of alumina-silicate proved as a superior material for various industrial applications. The specific advantage gained is cost-effective alumina-silicate hybrid adsorbent as an alternative to expensive commercial precursors and solvents. The characterization techniques confirmed the successful synthesis of the alumina-silicate hybrid. IR showed new hybrid (Al-O-Si) peak at 1102 cm^{-1}, SEM image showed hexagonal shaped structures stacked onto one another and created large void spaces between particles facilitated the adsorption process. It showed adsorption of 69% of Pb and 65% of Hg at optimum induced concentration i.e., 70 mg/L. The adsorption studies demonstrated removal efficiency attributed to coulombic interactions and participation of

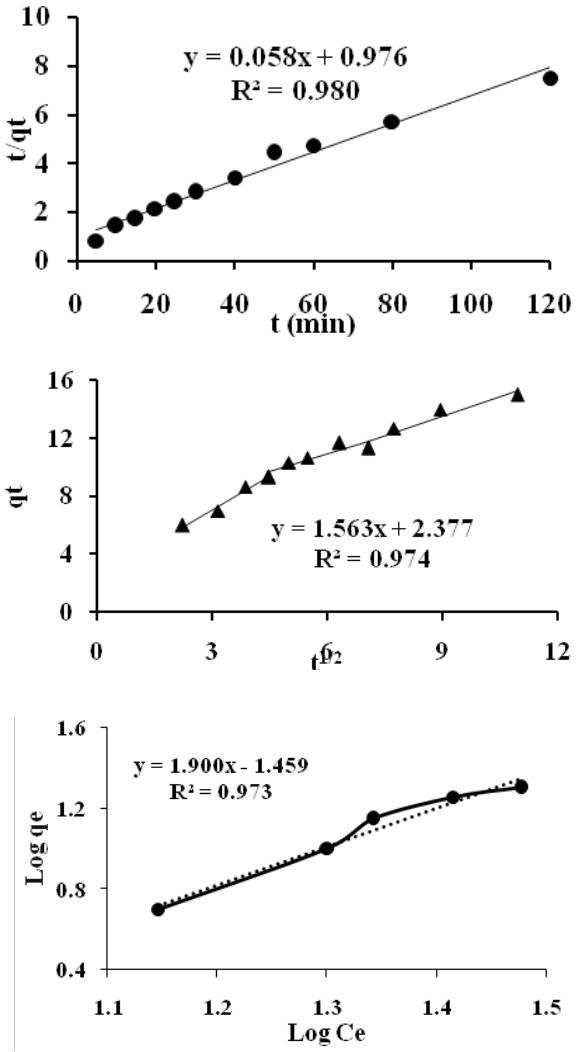

Fig. 8. Pseudo second order (a), intra particle diffusion (b) and Freundlich isotherm applied to Lead adsorption data at 70 mg/L.

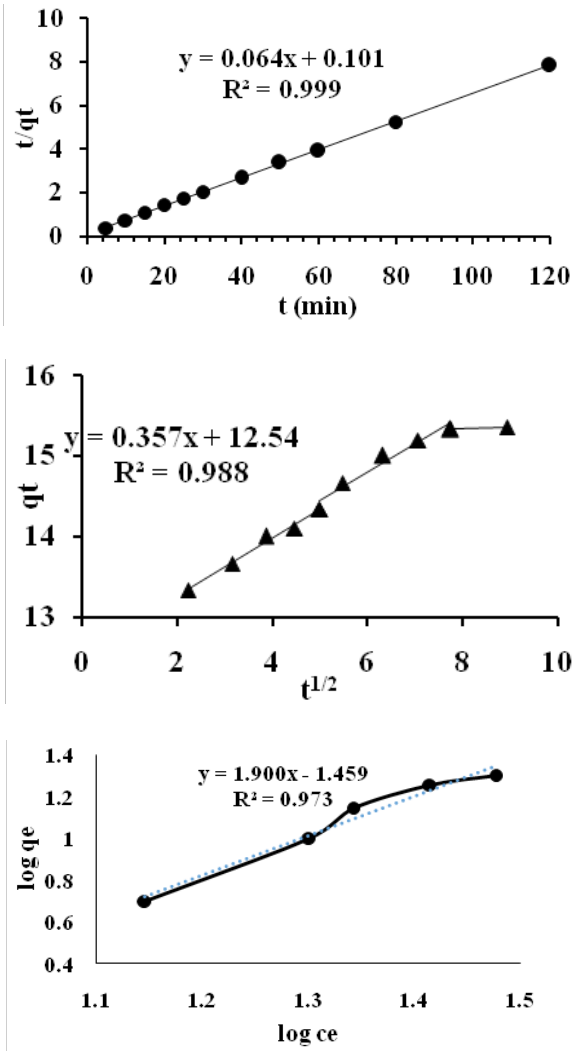

Fig. 9. Pseudo second order (a), intra particle diffusion (b) and Freundlich model applied to Mercury adsorption data at 70 mg/L.

Table 2
Kinetic parameter for the adsorption of Hg and Pb on alumina-silicate

Adsorption kinetics			
		Hg	Pb
	q_e exp. (µg/g and mg/g)	15.2	16
Pseudo-first order	K_1 (min^{-1})	1.1×10^{-2}	8.5×10^{-3}
	q_e cal. (mg/g)	2	10
	R^2	0.71	0.96
Pseudo-second order	K_2	2.3×10^2	3×10^2
	q_e cal. (µg/g and mg/g)	15.5	17
	R^2	0.99	0.98
Intraparticle diffusion	C_e cal. (mg/g)	3.5×10^{-2}	1.6×10^{-2}
	K_{id} (mg/g min)	12.5	5.9
	R^2	0.98	0.97
Adsorption Isotherms			
Langmuir	q_m	9.8	9.4
	K_L	2.4×10^{-2}	2.6×10^{-2}
	R^2	0.96	0.96
Freundlich	n	5.2×10^{-2}	4.8×10^{-1}
	K_F	29	45
	R^2	0.97	0.97

Na^+ ion exchanger within the alumina-silicate framework. Thus, this research work provided an alternate synthesis option replacing electrochemical anodization for alumina-silicate and used as a cost-effective adsorbent for remediation of toxic pollutants. In addition, it can also be used as a sensor for detection of nitro compounds and can conveniently be applied as a carrier for targeted and controlled drug delivery.

References

[1] S. Deng, M. Kurttepeli, D.J. Cott, S. Bals, S.C. Detavernier, Porous nanostructured metal oxides synthesized through atomic layer deposition on a carbonaceous template followed by calcination, J. Mater. Chem. A., 3 (2015) 2642–2649.

[2] X. Lin, N. Zhao, P. Yan, H. Hu, F.J. Xu, The shape and size effects of polycation functionalized silica nanoparticles on gene transfection, Acta Biomater., 11 (2015) 381–392.

[3] C.M. Lieber, Semiconductor nanowires: A platform for nanoscience and nanotechnology, MRS Bull., 36 (2011) 1052–1063.

[4] X. Qin, J. Zhang, J.X. Meng, L. Wang, C. Deng, G. Ding, X. Xu, Effect of ethanol on the fabrication of porous anodic alumina in sulphuric acid, Surf. Coat. Tech., 254 (2014) 398–401.

[5] D. Nakajima, T. Kikuchi, S. Natsui, R.O. Suzuki, Growth behaviour of anodic oxide formed by aluminum anodizing in glutaric and its derivative acid electrolytes, Appl. Surf. Sci., 321 (2014) 364–370.

[6] X. Chen, D. Yu, L. Cao, X. Zhu, Y. Song, H. Huang, X. Chen, Fabrication of ordered porous anodic alumina with ultra-large interpore distances using ultrahigh voltages, Mater. Res. Bull., 57 (2014) 116–120.

[7] S. Boulogne, J. Henderson, Indian glass in the Middle East? Medieval and Ottoman glass bangles from central Jordan, J. Glass Stud., 59 (2009) 53–75.

[8] Y. Yan, Y. Zhang, G. Meng, L. Zhang, Synthesis of ZnO nanocrystals with novel hierarchical structures via atmosphere pressure physical vapor deposition method, J. Cryst. Growth., 294 (2006) 184–190.

[9] Y. Wang, C. Bryan, H. Xu, P. Pohl, Y. Yang, C.J. Brinker, Interface chemistry of nanostructured materials: Ion adsorption on mesoporous alumina, J. Colloid Interface Sci., 254 (2012) 23–30.

[10] W. Cai, Y. Hu, J. Yu, W. Wang, J. Zhou, M. Jaroniec, Template free synthesis of hierarchical γ-Al_2O_3 nanostructures and their adsorption affinity toward phenol and CO_2, RSC Adv., 5 (2015) 7066–7073.

[11] S. Simon, M. Tămăşan, T. Radu, V. Simon, Doping and calcination effect on nanostructured aluminosilicates processed by sol-gel route, Eur. Phys. J. Appl. Phys., 55 (2011) 645–653.

[12] T.A. Saleh, Mercury sorption by silica/carbon nanotubes and silica/activated carbon: a comparison study, J. Water Supply Res. T., 64 (2015) 892–903.

[13] P.P. Nampi, P. Moothetty, F.J. Berry, M. Mortimer, K.G. Warrier, Aluminosilicates with varying alumina–silica ratios: synthesis via a hybrid sol–gel route and structural characterization, Dalton Trans., 39 (2010) 5101–5107.

[14] A.A.A.A. Gaber, D.M. Ibrahim, F.F. Abd-AImohsen, M.M. El-Zanati, Synthesis of alumina, titania, and alumina-titania hydrophobic membranes via sol gel polymeric route, Anal. Sci. Technol., 4 (2013) 18.

[15] F. Tariq, U. Rafique, K. Yaqoob, Synthesis of alumino-silicates functionalized titanium as potential adsorbent: An industrial possibility, EpitoanyagJ. Silica. Comp. Mater., 3 (2017) 94–97.

[16] J.M. Silva, E.B. Silveira, A.L. Costa, C.O. Veloso, C.A. Henriques, F.M. Zotin, S.S. Chiaro, Influence of the chemical composition of silica – alumina adsorbents in sulfur and nitrogen compounds removal from hydrotreated diesel, Ind. Eng. Chem. Res., 53 (2014) 16000–16014.

[17] M. Jung, NMR characterization on the preparation of sol–gel derived mixed oxide materials, Int. J. Inorg. Mater., 3 (2001) 471–478.

[18] S. Music, N. Filipovic-Vincekovic, L. Sekovanic, Precipitation of amorphous SiO_2 particles and their properties, Braz. J. Chem. Eng., 28 (2011) 89–94.

[19] K. Parveen, U. Rafique, S. Safi, M.A. Ashraf, A novel method for synthesis of functionalized hybrids and their application for wastewater treatment, Desal. Water Treat., 57 (2016) 161–170.

[20] A. Adamczyk, The structural studies of aluminosilicate gels and thin films synthesized by the sol-gel method using different Al_2O_3 and SiO_2 precursors, Mater. Sci-Poland., 33 (2015) 732–774.

[21] M. Todea, R.V.F. Turcu, B. Frentiu, M. Tamasan, H. Mocuta, O. Ponta, S. Simon, Amorphous and nanostructured silica and aluminosilicate spray dried microspheres, J. Mol. Struct., 1000 (2011) 62–68.

[22] A.A. Warra, Transition metal complexes and their application in drugs and cosmetics – A Review, J. Chem. Pharm. Res., 3 (2011) 951–958.

[23] J. Peric, M. Trgo, N.V. Medvidović, Removal of zinc, copper and lead by natural zeolite—a comparison of adsorption isotherms, Water Res., 38 (2004) 1893–1899.

[24] P. Schneider, Adsorption isotherms of microporous-mesoporous solids revisited, Appl. Catal. A., 129 (1995) 157–165.

[25] D. Macina, Z. Piwowarska, K. Tarach, K. Góra-Marek, J. Ryczkowski, L. Chmielarz, Mesoporous silica materials modified with alumina polycations as catalysts for the synthesis of dimethyl ether from methanol, Mater. Res. Bull., 74 (2016) 425–435.

[26] M. Liu, L. Hou, B. Xi, Y. Zhao, X. Xia, Synthesis, characterization and mercury adsorption properties of hybrid mesoporous aluminosilicate sieve prepared with fly ash, Appl. Surf. Sci., 273 (2013) 706–716.

[27] A. Mudhoo, K. Vinod, K.V. Garg, S. Wang, Removal of heavy metals by biosorption, Environ. Chem. Lett., 10 (2012) 109–117.